Inhibition of hydrogen oxidation by HBr and Br_2

Graham Dixon-Lewis[a,1], Paul Marshall[b], Branko Ruscic[c], Alexander Burcat[d], Elke Goos[e], Alberto Cuoci[f], Alessio Frassoldati[f], Tiziano Faravelli[f], and Peter Glarborg[g]

a: Department of Fuel and Energy, University of Leeds, Leeds LS2 9JT, UK
b: Department of Chemistry and Center for Advanced Scientific Computing and Modeling (CASCaM), University of North Texas, Denton, 1155 Union Circle #305070, Texas 76203–5017
c: Chemical Sciences and Engineering Division, Argonne National Laboratory, Argonne, Illinois 60439, USA
d: Faculty of Aerospace Engineering, Technion–Israel Institute of Technology, Haifa 32000, Israel
e: Institute of Combustion Technology, DLR, D-70569 Stuttgart, Germany
f: Dipartimento di Chimica, Materiali e Ingegneria Chimica "G. Natta", Politecnico di Milano, P.zza Leonardo da Vinci 32, 20133 Milano, Italy
g: DTU Chemical Engineering, Technical University of Denmark, 2800 Lyngby, Denmark

---

Abstract

The high-temperature bromine chemistry was updated and the inhibition mechanisms involving HBr and Br_2 were re-examined. The thermochemistry of the bromine species was obtained using the Active Thermochemical Tables (ATcT) approach, resulting in improved data for, among others, Br, HBr, HOBr and BrO. Ab initio calculations were used to obtain rate coefficients for selected reactions of HBr and HOBr, and the hydrogen/bromine/oxygen reaction mechanism was updated. The resulting model was validated against selected experimental data from literature and used to analyze the effect of HBr and Br_2 on laminar, premixed hydrogen flames. Our work shows that hydrogen bromide and molecular bromine act differently as inhibitors in flames. For HBr, the reaction HBr + H $\rightleftharpoons$ H_2 + Br (R2) is rapidly equilibrated, depleting HBr in favor of atomic Br, which is the major bromine species throughout the reaction zone. The chain-breaking

[1]Deceased 5 August 2010

steps are then H + Br + M → HBr + M (R1), Br + HO_2 → HBr + O_2 (R7), and Br + Br + M → Br_2+M (R8). In Br_2-doped flames, the reaction Br_2 + H ⇌ HBr + Br (R9) is far from equilibration and serves to deplete H in the reaction zone by competing with H + O_2 → O + OH. The inhibition is augmented by recombination of Br (R8). If the inlet Br_2 mole fraction exceeds about 20%, reactions (R8) and (R2) are both reversed, now acting to promote chain branching and increase the flame speed. According to the present model, cycles involving HOBr are not important for generation or removal of chain carriers in these flames.

Introduction

Bromine reactions are important in stratospheric chemistry where, on a per atom basis, bromine is considerably more active in depleting ozone than chlorine [1]. Despite recent regulations, brominated flame retardants are still an ingredient in many materials, and bromine reactions continue to be a concern in relation to waste incineration processes [2, 3]. Due to the interaction of bromine species with the combustion process and with other trace species, there is a renewed interest in the elementary reactions of bromine species, in particular at higher temperatures [4]. The presence of bromine species may enhance or inhibit fuel oxidation, depending on the reaction conditions [5]. This behavior is similar to that reported for trace elements naturally occurring in combustion, e.g. N, S, Cl, and K/Na [6]. In flames, bromine appears to be the most effective halogen inhibitor, and bromine species have been reported to narrow the composition limits of inflammability [7–11] and to decrease flame speeds [12–19]. The inhibiting effect of bromine species has also been observed at lower temperatures in batch reactor [20, 21] and flow reactor [22] experiments. However, static reactor experiments have shown that hydrogen bromide acts to catalyze the slow oxidation of hydrocarbons [5, 23–29].

Despite the considerable interest in high-temperature bromine reactions, details of the chemistry remain uncertain. Most bromine reactions have only been characterized experimentally at low temperatures, if at all, and bromine reaction mechanisms have not been validated over a wider range of conditions. The first computational studies of the inhibiting effect of bromine species in flames were conducted by Dixon-Lewis and coworkers [30–32] for premixed hydrogen–air flames and later by Westbrook for hydrocarbon flames [33, 34]. These early studies dealt mainly with HBr and Br_2 as inhibitors. More recent chemical kinetic studies of the interaction of bromine species with combustion chemistry have emphasized CF_3Br and related halogens [19, 22, 34–39].

It is known that even for brominated hydrocarbons and commercial inhibitors such as CF_3Br (Halon 1301), the active species in the radical removal cycles are mainly HBr and Br, together with CH_3Br [14, 16, 22, 35, 40]. However, the earlier studies of the Br/H/O system and the effects of bromine on combustion were limited by incomplete data for thermodynamic properties of some

of the potentially important bromine species, as well as uncertainties in the rate constants of many of the steps involved in the inhibition. The objective of the present work is to update our knowledge of the high-temperature bromine chemistry and re-examine the inhibition mechanisms involving HBr and Br_2. The thermochemistry of the bromine species is re-examined and the hydrogen/bromine/oxygen reaction mechanism is updated, partly based on *ab initio* calculations for key reactions. The resulting model is validated against selected experimental data from literature and used to analyze the effect of HBr and Br_2 on laminar, premixed hydrogen flames.

Thermochemistry

The thermochemistry of the bromine-containing species of interest, given in Table 1, was obtained using the Active Thermochemical Tables (ATcT) approach [41,42], which, in contrast to the traditional "sequential" approach, derives accurate, reliable, and internally consistent thermochemical values by analyzing and simultaneously solving [43–45] all the available thermochemical interdependencies defined in the underlying Thermochemical Network (TN) [46,47]. The most recent ATcT TN (ver. 1.110) [45,48], which contains more than 13000 thermochemical determinations encompassing over 900 chemical species, has been expanded and updated (ver. 1.112) to accommodate the targeted bromine-containing species. The resulting ATcT values have been in turn used to update the database of Goos, Burcat, and Ruscic [49,50] with the appropriate polynomials.

Under the auspices of CODATA, Br_2, Br, and HBr, were established as "key" thermochemical species by Cox et al. [51], and the gas-phase enthalpies of formation that were derived by critical evaluation of data available up to (approx.) 1983, $\Delta_f H^0_{298}(Br_2) = 30.91 \pm 0.11$ kJ mol^{-1}, $\Delta_f H^0_{298}(Br) = 111.87 \pm 0.12$ kJ mol^{-1}, and $\Delta_f H^0_{298}(HBr) = -36.29 \pm 0.16$ kJ mol^{-1}, have been adopted without further scrutiny by virtually all subsequent thermochemical tabulations. For gaseous Br_2 (the formation enthalpy of which is equivalent to the vaporization enthalpy of condensed-phase bromine corrected for ideal vs. real behavior) there are indeed no relevant measurements since the evaluation of Cox et al. However, for Br and HBr, there are several newer determinations that can potentially improve and/or modify the thermochemistry of

these two "key" species, such as, for example, the analysis of spectroscopic data by Gerstenkorn and Luc [52] leading to a refined value of $D_0(Br_2)$, or the spectroscopic determination of predissociation of HBr^+ [53] that allows access to $D_0(HBr)$ via a positive ion cycle. Thus, the current ATcT value for Br (unchanged from the value in the very recently given interim set of ATcT enthalpies of formation of several atoms [45]; enthalpy of formation at 298.15 K of 111.85±0.06 kJ mol^{-1}, while confirming the original CODATA value [51], is actually more accurate by a factor of two. The agreement for Br is not replicated in the case of HBr. The original CODATA value for HBr is essentially based on the assigned value for aqueous Br^- and the selected solvation enthalpy of HBr. In contrast to this, the ATcT TN - while also containing the relevant aqueous thermochemistry -takes advantage of newer thermochemical cycles that are entirely gas-phase. Consequently, ATcT currently produces an enthalpy of formation of HBr (-35.85±0.15 kJ mol^{-1} at 298.15 K) that is higher (less negative) than the value assigned by CODATA by an amount that - while not large in absolute terms - exceeds substantially the combined uncertainties, leading to the conclusion that the aqueous thermochemical route selected by CODATA contains a hidden cumulative systematic bias that is larger than their declared uncertainty. It should be stressed here that while the current ATcT value for HBr relies heavily on spectroscopic data, it is, at the same time, still entirely consistent (within the respective uncertainties) with the relevant calorimetric [54, 55] and aqueous [56–64] thermochemical measurements.

For BrO, the ATcT TN contains a number of experimental determinations that are relevant to defining its D_0 [65–71]. These are complemented by the results of several high-level electronic structure computations [72–78], which, if and when possible, were recast as congeneric reactions, adding within the TN relevant interdependences between various haloxyl radicals and/or their ion counterparts (halosyls and hypohalites). The resulting ATcT value for the enthalpy of formation of BrO (123.6±0.3 kJ mol^{-1} at 298.15 K) is about 2 kJ mol^{-1} lower and nearly an order of magnitude more accurate than the value given by JANAF [79] and Gurvich et al. [80] (both report 125.8±2.4 kJ mol^{-1}).

Good definition of the thermochemistry of the basic bromine-containing species discussed briefly above is a prerequisite for deriving with some confidence the thermochemistry of HOBr, which potentially plays a pivotal role

in the chemical processes presented in this study. The often-cited lower limit for the enthalpy of formation of HOBr at 298.15 K of -56.2±1.8 kJ mol^{-1} given by Ruscic and Berkowitz [81] is based on their determination of the photoionization onset for fragmentation into Br^+ and OH. However, two complications regularly seem to escape focus. Firstly, the limiting value derived from that particular photodissociative onset intrinsically depends, inter alia, on the choice for the enthalpy of formation of OH. Ruscic and Berkowitz have taken the latter from Gurvich et al. [80], which was the best datum available at that time. Ruscic et al. [82, 83] have subsequently shown that $\Delta_f H^0(OH)$ needs to be revised downward by about 2 kJ mol^{-1}. The implication is that the limiting value of Ruscic and Berkowitz [81] should also be then revised accordingly. With auxiliary thermochemical data extracted from the current version of ATcT, the limit of Ruscic and Berkowitz, revised in light of the change for OH, would correspond to -58.0±1.8 kJ mol^{-1}. A second complication is related to the generally assumed rigidity of the "limit". Prima facie, photoionization onsets are indeed expected to be strict upper limits, placing an upper limit on the sum of the enthalpies of formation of the products or (in this case) a lower limit on the enthalpy of formation of the parent. However, Ruscic and Berkowitz discuss at some length a substantial complication: their recorded photoionization spectrum of Br^+ is from a mixture of HOBr and Br_2, the latter having a significantly lower onset for photodissociative ionization to produce the monitored ion Br^+ than the former (by 0.169 eV, according to current ATcT results). While Ruscic and Berkowitz attempted to find a method of production of HOBr that will minimize the unwanted Br_2 component, the final spectrum nevertheless required a subtraction of the Br^+ signal from Br_2. Clearly, such a subtraction of a secondary (and lower energy) source of the same signal will tend to vitiate the rigidity of the limit. Luckily, since the studies of HOBr by Ruscic and Berkowitz [81, 84], there are several new experimental and theoretical determinations relevant to its thermochemistry, such as kinetic rate constant studies of Monks et al. [85] and Kukui et al. [86] that complement earlier data by Loewenstein and Anderson [87], the photodissociation study of Lock et al. [88], and the computational results by Lee [89], Glukhovtsev et al. [90], Hassanzadeh and Irikura [78], Ren et al. [91], and Denis [92]. All of these are included in the TN, resulting in the current ATcT value of $\Delta_f H^0_{298}(HOBr)$ = -61.8±0.6 kJ mol^{-1}. This value is, in fact, somewhat lower than the (revised) lower limit of Ruscic and Berkowitz, and is relatively similar to the recent evaluation of

Hassanzadeh and Irikura (-60.5±1.1 kJ mol^{-1}).

With respect to gas phase BrOBr, there are only two experimental determinations of thermochemical relevance: Orlando and Burkholder [93] determined the equilibrium constant between BrOBr, water, and HOBr, and Thorn et al. [94] measured the photoionization fragmentation onset of BrO+ from BrOBr; for the remaining triatomic bromine oxides (BrOO, OBrO, BrBrO) there are essentially no earnest experimental thermochemical determinations. The paucity of experimental data is compounded by the fact that these species tend to seriously strain the electronic structure methods and their results need to be taken with some caution. The available basis sets for Br pose a serious constraint on the fidelity of state-of-the-art theoretical computations. This is further complicated by the fact that even higher order relativistic effects are far from being negligible and generally need to be explicitly computed. In addition, single-reference methods (which may, at least in principle, attain chemical accuracy) suffer from severe spin-contamination for BrOO and in general produce unusable results. The ATcT values for the triatomic bromine oxides, given in Table 1, are based on the two mentioned experimental determinations related to BrOBr and the best available theoretical results [74, 89, 95–98], which were also included in the TN.

Ab Initio Calculations

A number of potentially important reactions in the bromine mechanism have not previously been characterized experimentally. These include the reaction of HBr with HO_2 and a number of steps involving HOBr. In order to provide more reliable values for the rate constants of these reactions, we have conducted ab initio calculations. Geometries of stationary points, and vibrational frequencies scaled by a factor of 0.967, were obtained using density functional theory with the Gaussian09 program suite [99]. All-electron B3LYP/6-311+G(d,p) values were derived. Geometries and frequencies for the transition states are given in Fig. 1. Single-point energies were obtained using spin-unrestricted coupled cluster theory implemented with Molpro 2009 [100], using the cc-pVTZ and cc-pVQZ basis sets. For bromine the core electrons were represented via an effective core potential (cc-pVnZ-PP basis sets) which partially allows for scalar relativistic effects. These

CCSD(T) results were extrapolated to the infinite basis set limit via the $1/n^3$ relation of Halkier et al. [101] and with the inclusion of vibrational zero-point energy yield relative enthalpies at 0 K. The data, summarized in Table 2, were employed in canonical transition state theory calculations, using the rigid-rotor and simple harmonic oscillator approximations, with Wigner tunneling corrections.

The reaction

$$HBr + HO_2 \rightleftharpoons Br + H_2O_2 \qquad (R5)$$

has been studied in both the forward and reverse directions at lower temperatures, but with a single exception only upper limit values have been reported. In the forward direction, Mellouki et al. [102] reported k_5 to be smaller than 1.8 x 10^7 and 2.7 x 10^8 cm^3 mol^{-1} s^{-1} at 300 and 400 K, respectively. In the reverse direction, the most stringent upper limit is $k_{5b}(378\ K) < 3.0$ x 10^8 cm^3 mol^{-1} s^{-1} [103]. The rate constant for (R5b) reported by Heneghan and Benson [104] is in conflict with the upper limits reported in the other low-temperature studies.

At higher temperatures, there are only indirect results available for the reaction. A reaction between HBr and HO_2 (R5) is supported by batch reactor results on the HBr/O_2 reaction system [14, 105–107], but specific values for k_5 were not reported. Clark et al. [21] found that Br + H_2O_2 (R5b) was important to explain the effect of HBr on the second explosion limit of the H_2/O_2 system. They derived a value of $k_{5b}(773\ K) \approx 10^{11}$ cm^3 mol^{-1} s^{-1}.

From theory we calculate a rate constant for HBr + HO_2 of $k_5 = 4.2$ x 10^2 $T^{2.93}$ exp(-3861/T) cm^3 mol^{-1} s^{-1}. In Fig. 2, this value is compared with data reported in literature. Except for the results of Heneghan and Benson, the calculated k_5 is in agreement with other studies, being well below the upper limits reported at lower temperatures [102, 103, 108, 109]. Our rate constant is an order of magnitude lower than the value reported by Clark et al. [21] at 773 K, but our present modeling of their results, discussed below, shows little sensitivity to the value of k_5.

In the present work, special attention was paid to reactions of HOBr. For the thermal dissociation of HOBr,

$$HOBr(+M) \rightleftharpoons Br + OH(+M) \qquad (R19)$$

our estimate based on Troe's formalism [110] for the low-pressure limit is $k_{19,0}$ = 1.3 x 10^{22} $T^{-1.52}$ exp(-25667/T) cm^3 mol^{-1} s^{-1}. The rate constant for the high-pressure limit, $k_{19,\infty}$ = 1.0 x 10^{15} exp(-24500/T) s^{-1} is only a rough estimate made from analogy with other simple bond-fission reactions, but under the conditions of the present study the reaction is at or close to the low-pressure limit.

The HOBr + H reaction has three product channels,

$$HOBr + H \rightleftharpoons BrO + H_2 \quad \text{(R20)}$$

$$HOBr + H \rightleftharpoons HBr + OH \quad \text{(R21)}$$

$$HOBr + H \rightleftharpoons Br + H_2O \quad \text{(R22)}$$

For the first channel over 298-2000 K, we get essentially the same barrier as computed in the literature for the Cl analogue [111,112]. The calculated rate constant is k_{20} = 2.0 x 10^7 $T^{1.91}$ exp(-4032/T) cm^3 mol^{-1} s^{-1}. We find no barrier to the other two channels; both reactions are presumably very fast (for the analogous HOCl channels there are moderate 4-16 kJ mol^{-1} barriers instead). Under conditions, where HOBr is formed in significant quantities, the branching fraction between (R21) and (R22) may become important, but a reliable estimate of the ratio will require a more detailed study.

Similar to HBr + HO_2 (R5), the reaction between HOBr and HO_2

$$HOBr + HO_2 \rightleftharpoons BrO + H_2O_2 \quad \text{(R25)}$$

is comparatively slow. We get k_{25} = 1.03 $T^{3.55}$ exp(-6590/T) cm^3 mol^{-1} s^{-1}.

Reaction Mechanism

The chemical kinetic model used in the present study consists of a H_2 oxidation scheme together with a subset for the Br/H/O system. The H_2/O_2 reaction system has been analyzed in a number of recent comprehensive kinetic studies [113–118]. Even though there are consensus values for many of the key reactions in the hydrogen oxidation mechanism, there are still unresolved issues [119] and modeling predictions of important parameters such as explosion limits and flame speeds vary among the proposed schemes. In

the present work, we have adopted the mechanism of Rasmussen et al. [118], updating the rate coefficients for the recombination reactions of H with OH and with O_2 from the recent theoretical study of Sellevag et al. [120]. Even though the remaining uncertainties, e.g. in the peroxide subset, influence the calculations presented in this work, they do not affect the conclusions made on the inhibiting mechanisms of bromine.

The bromine subset is an update of the mechanism developed by Babushok and coworkers [36, 37] to describe flame inhibition by CF_3Br. The thermodynamic properties for bromine species were adopted from the Ideal Gas Thermochemical Database by Goos, Burcat and Ruscic [49], with updates from Active Thermochemical Tables, as described above. The transport coefficients for use in flame modeling were drawn from Noto et al. [37].

The bromine subset of the reaction mechanism is listed in Table 3. Compared to the work of Babushok and coworkers [36, 37], a number of rate constants have been updated and a few reactions involving HOBr and BrOO were added. Where possible, the rate constants were drawn from data evaluations [121, 123, 124]. However, a number of potential key reactions were characterized by transition state theory, as discussed above.

Despite the interest for bromine species as flame inhibitors, most of the work on elementary reactions have been conducted at lower temperatures. The key steps in the H_2/Br_2 system, i.e.

$$H + Br + M \rightleftharpoons HBr + M \tag{R1}$$

$$HBr + H \rightleftharpoons Br + H_2 \tag{R2}$$

$$Br + Br + M \rightleftharpoons Br_2 + M \tag{R9}$$

$$Br_2 + H \rightleftharpoons HBr + Br, \tag{R10}$$

are among the reactions characterized over a wider temperature range. For these reactions, the preferred rate coefficients [121, 122] were derived from direct low temperature measurements in combination with interpretation of results from batch reactors and shock tubes.

A key chain-breaking step in bromine-inhibited combustion is believed to be the reaction between atomic bromine and the HO_2 radical [21, 30],

$$Br + HO_2 \rightleftharpoons HBr + O_2 \tag{R7}$$

The rate constant for this reaction has been measured directly at low temperatures and by indirect means at higher temperatures. Atkinson et al. [124] review the available low-temperature data and base their recommendation on the data from Toohey et al. [103], Laverdet et al. [128], and Bedjanian et al. [129], which are all in acceptable agreement. The observed kinetics are consistent with the mechanism proceeding via direct hydrogen atom abstraction to yield HBr, as also indicated by theoretical studies of the reaction [130].

At the higher temperatures of interest in the present work, only indirect measurements have been reported. In the forward direction, Dixon-Lewis and coworkers [30] estimated a value at 1000 K from data on the effect of HBr on the flame speed [30] of H_2/air mixtures. Similarly, Clark et al. [21] reported a value of k_7 at 773 K based on data on the effect of HBr on the second explosion limit [21] of the H_2/O_2 system. Values for the reverse rate constant k_{7b} for the HBr + O_2 reaction have been obtained from batch reactor experiments on HBr oxidation by O_2 at temperatures of 658-873 K [14, 105, 106]. Under these conditions the overall reaction is first order both in [HBr] and [O_2]. There is some scatter in the batch reactor data, which rely on interpreting a complex kinetic system that conceivably is also affected by reactions on the reactor surface [107].

Figure 3 shows an Arrhenius plot for reaction (R7). Here, the measurements for k_7 are compared with data for the reverse step, converted through the equilibrium constant for the reaction. We have extrapolated the low-temperature results, assuming a weak non-Arrhenius curvature in the rate constant. The resulting rate coefficients provide a good description of the direct measurements and agree within the uncertainty with most of the data reported at higher temperatures. However, it is noteworthy that the data by Clark et al. support a stronger temperature dependence, as discussed below, and it is desirable to have a direct measurement of the reaction rate at higher temperatures.

Only few of the other bromine reactions listed in Table 3 have been measured above 500 K. However, many of the reactions have a small or negligible activation barrier, and results derived at low temperatures can be extrapolated with some confidence to high temperatures. The HBr+OH reaction (R4) has an unusual temperature dependence at very low temperatures, but its rate constant is independent of temperature above 200 K [131].

In the present work, we have paid particular attention to the reactions involving HOBr. A chain terminating sequence involving HOBr, such as

$$\mathrm{Br + OH(+M) \rightleftharpoons HOBr(+M)} \qquad \text{(R19b)}$$

$$\mathrm{HOBr + H \rightleftharpoons Br + H_2O} \qquad \text{(R22)}$$

$$\mathrm{Br + HO_2 \rightleftharpoons HBr + O_2,} \qquad \text{(R7)}$$

could possibly constitute an active inhibitive cycle. HOBr was not considered in the early work on flame inhibition by bromine species. In more recent work, Babushok and coworkers [36, 37] used an estimated low-pressure limit rate constant for (R19), which is much smaller than the current RRKM value, effectively shutting off cycles initiated by (R19b).

In the past, rate constants for HOBr reactions have been estimated by analogy with chlorine reactions. Even though this analogy works well for a number of Br/Cl reactions, it should be used cautiously. For HOBr, only the reaction with atomic O (R23) has been measured directly [124]. It is noteworthy that this reaction is about two orders of magnitude faster than the corresponding reaction of HOCl. In addition to k_{20}, we have determined rate constants for HOBr+H and HOBr+HO_2 from ab initio calculations (see above), while data for HOBr+OH were drawn from a recent theoretical study by Wang et al. [127] (Table 3).

The most uncertain part of the mechanism involves reactions of BrOO; rate constants are only rough estimates. However, because of the low thermal stability of this peroxide, the uncertainties associated with the BrOO reactions have no impact on the modeling predictions. Table 1 gives a Br–OO bond strength of 1.7 ± 3.9 kJ mol^{-1}, which is essentially zero. Therefore [BrOO] should be zero and it is doubtful whether it can be considered as a species.

Results and Discussion

Earlier experimental results on the H_2/Br_2 chemistry at high temperatures include data for laminar flame speeds [132–135], flame structure [136], shock tube results [137–139], and flow reactor results [140]. The H_2/Br_2 system is conceptually simple, involving primarily the chain propagating steps, Br +

$H_2 \rightleftharpoons HBr + H$ (R2b) and $Br_2 + H \rightleftharpoons HBr + Br$ (R10), as well as dissociation / recombination reactions involving Br_2 (R9), HBr (R1) and H_2.

Figure 4 shows a comparison between the measurements of Frazier et al. [136] and modeling predictions for the structure of a spherical, low-pressure H_2/Br_2 flame. The flame had an initial content of 44.2% bromine and a pressure of 0.117 atm. The modeling predictions are in reasonable agreement with the experimental data. The H_2 concentration is predicted quantitatively, while Br_2 and HBr profiles are slightly shifted. The use of a measured temperature profile in the calculations puts restrictions on the modeling, and uncertainties in the temperature will affect also the accuracy of the predictions.

A more severe test of the H_2/Br_2 mechanism is the prediction of burning velocities for H_2/Br_2 mixtures. Figure 5 compares measured laminar flame speeds for H_2/Br_2 by Cooley and coworkers [132–134] with modeling predictions. The measurements were conducted on different setups, using Bunsen type burners as well as tubes, and with a range of different techniques, and there are some scatter in the data. The modeling predictions are seen to be in good agreement with the experiments; in particular with the early measurements [132, 133], which we consider to be most reliable.

Figure 6 shows the linear sensitivity coefficients for the predicted flame speed for three H_2/Br_2 ratios. According to this analysis, the predictions are most sensitive to the rate constant of the initiation step,

$$Br_2 + M \rightleftharpoons Br + Br + M \qquad \text{(R8b)}$$

and the two chain-propagating steps,

$$Br + H_2 \rightleftharpoons HBr + H \qquad \text{(R2b)}$$

$$Br_2 + H \rightleftharpoons HBr + Br, \qquad \text{(R9)}$$

All these reactions exhibit positive sensitivity coefficients, while the chain terminating step,

$$H + Br + M \rightleftharpoons HBr + M \qquad \text{(R1)}$$

shows a small negative sensitivity. The good agreement between measurements and modeling predictions confirms that this part of the bromine mechanism is well established.

The introduction of oxygen in the hydrogen/bromine system increases the chemical complexity substantially. Unfortunately, experimental data on the H/Br/O chemistry at medium to high temperatures are limited. Reported results are largely limited to data on the effect of HBr on the H_2/O_2 system, i.e. explosion limits [20, 21], flammability limits [30] and flame speeds [17, 18]. Among the data obtained at medium temperatures, we have chosen to emphasize the batch reactor results from Clark et al. [21]. To our knowledge, these data constitute the most detailed experimental study that has been reported on the effect of bromine species on hydrogen oxidation.

Clark et al. investigated the inhibition of the second explosion limit of the hydrogen–oxygen reaction by HBr in a batch reactor at 773 K. Gas mixtures of H_2, O_2, and N_2, with or without HBr, were premixed in specific ratios at a pressure greater than the second explosion limit. Gases were then withdrawn from the vessel until explosion occurred. Clark et al. optimized the withdrawal rate to ensure that stationary conditions were obtained. The H_2/O_2 ratio was varied from 0.15 to 4, while HBr was added in amounts from 0 to 600 ppm (balance N_2).

Even though the results of Clark et al. were reported to be independent of the surface/volume ratio of the reactor, the condition of the vessel surface remains a concern. For example a strongly chain breaking surface such as KCl will remove all HO_2 reaching it, with the result that HO_2, once formed, does not react further before it is destroyed. In this way the principal chain terminating property of atomic Br would be by-passed and the effect of HBr on the limit would not be likely to be large. However, comparison of the results of Clark et al. for the undoped experiments with modeling predictions with the present mechanism indicates that loss of HO_2 is small or negligible.

Figure 7 compares selected experimental results of Clark et al. with modeling predictions with the present mechanism. Here, the inlet H_2 concentration was maintained at 28%, while O_2 was varied in the range 7-56%. The data indicate that at low levels of HBr addition, the explosion limit varies with the H_2/O_2 ratio. However, as the HBr concentration increases above 200 ppm, the explosion limit becomes independent on the H_2/O_2 ratio over the range investigated and depends solely on [HBr].

The second explosion limit is primarily governed by the competition between

the reactions

$$H + O_2 \rightarrow O + OH$$

$$H + O_2 + M \rightarrow HO_2 + M$$

and subsequent loss of HO_2. The prediction of the explosion limit was sensitive to the choice of criterion (here chosen as the onset of rapid reaction within 10 s), but the H_2/O_2 explosion limits were predicted satisfactorily over a range of ratios and without including surface loss of species, just by a small adjustment to the collision efficiency of N_2 in the H+O_2(+M) reaction.

The model describes the results for the H_2/O_2/HBr system qualitatively correctly, but underestimates the inhibiting effect of HBr, most pronounced at low doping levels. According to the calculations, addition of HBr leads to chain termination through the reactions

$$HBr + H \rightleftharpoons Br + H_2 \qquad \text{(R2)}$$

$$Br + HO_2 \rightleftharpoons HBr + O_2 \qquad \text{(R7)}$$

Clark et al. [21] attributed the observed reduction of the pressure limit to HO_2 radical removal by reaction with Br. This is confirmed by a sensitivity analysis that identifies (R7) as the single most important chain-breaking step at all conditions investigated. Chain-breaking cycles involving HOBr are not significant, according to the present model.

Clark et al. used an elementary reaction mechanism to interpret their data. From their analysis, they were able to derive rate constants for reactions (R7) and (R8) at 773 K. However, their model contained a number of deficiencies. For instance, their reaction mechanism included the chain-propagating reaction H+HO_2 $\rightleftharpoons$ OH+OH, but not the terminating step H+HO_2 $\rightleftharpoons$ H_2+O_2. In addition, a number of the rate constants in their scheme are now known to be inaccurate. Still, the present analysis confirms that the best agreement between modeling predictions and experimental data is obtained with their estimated ratio of $k(H+HO_2=OH+OH)/k_7 = 8.0 \pm 1.6$ at 773 K. With the current rate constant for H+HO_2, this corresponds to a value of k_7(773 K) of 8.1 x 10^{12} cm^3 mol^{-1} s^{-1}, considerably higher than the value of about 5 x 10^{12} cm^3 mol^{-1} s^{-1} recommended by Clarke et al. (see Fig. 3) and used in the present work. The high value is not supported by other measurements, but a direct determination of k_7 at higher temperatures is desirable.

Contrary to the assumption of Clark et al., our analysis indicates that the reaction between Br and H_2O_2 (R8) play at most a small part in this chemistry. The present modeling predictions of the explosion limit do not show sensitivity to the value of k_8, even with a much higher value than calculated from our ab initio calculation (see above) and the derivation Clarke et al. of $k_8(773\ \mathrm{K}) \approx 10^{11}\ \mathrm{cm^3\ mol^{-1}\ s^{-1}}$ cannot be confirmed by our modeling.

Laminar premixed flames are less prone to surface effects than experiments conducted in batch reactors. Unfortunately, there are only few experimental results available on the impact of HBr addition on the flame speed of hydrogen–air mixtures. Miller et al. [17] and Drake and Hastie [18] have reported burning velocities of fuel-rich H_2/air flames with and without addition of HBr, while Day et al. [30] investigated the effect of HBr addition on $H_2/O_2/N_2$ flames close to the rich flammability limit.

Figure 8 compares the experimental results of Day et al. [30] with modeling predictions. They investigated the effect of addition of very small quantities of HBr on the flame speed of $H_2/O_2/N_2$ close to the rich flammability limit. As shown in the figure, the burning velocity of the uninhibited mixture was measured to be 9.2 cm $\mathrm{sec^{-1}}$. Addition of a few hundred ppm of HBr lowered the flame speed by about 25%.

The model predicts flame speeds about 5 cm $\mathrm{sec^{-1}}$ higher than observed by Day et al., possibly due to uncertainties in the experimental values and/or the HO_2 subset of the mechanism. As reported by Day et al., modeling predictions are sensitive to the fate of HO_2, and very recent shock tube results [141] indicate that some of the rate constants in the HO_2/H_2O_2 subset of our mechanism may be inaccurate. However, in the present work no modifications were made to improve predictions.

Figure 9 shows sensitivity coefficients for the conditions of Fig. 8 and addition of 0, 250 and 500 ppm HBr, respectively. With a peak temperature below 1100 K, the undoped flame structure is sensitive to reactions of the HO_2 radical. The predicted flame speed is controlled by competition between the chain-branching and association channels of the H + O_2 reaction,

$$\mathrm{H + O_2 \rightleftharpoons O + OH}$$

$$\mathrm{H + O_2(+M) \rightleftharpoons HO_2(+M)},$$

as well as by the fate of HO_2; i.e., whether HO_2 + H is propagating or chain terminating

$$HO_2 + H \rightleftharpoons OH + OH$$

$$HO_2 + H \rightleftharpoons H_2 + O_2.$$

The presence of HBr introduces a number of chain breaking steps that serve to reduce the flame speed,

$$H + Br + M \rightleftharpoons HBr + M \tag{R1}$$

$$Br + HO_2 \rightleftharpoons HBr + O_2 \tag{R7}$$

It is noteworthy that only atomic bromine, not hydrogen bromide, is involved in the flame inhibition. This phenomena was explained in previous work by Dixon-Lewis and coworkers [30–32]. In a sequence of computational studies, they investigated the inhibiting effect of hydrogen bromide in premixed hydrogen–air flames. One of their interesting findings was that HBr virtually disappeared before the main reaction zone in these flames. This is confirmed by the predicted structure for the conditions of the 250 ppm HBr flame of Day et al., shown in Fig. 10. The reaction

$$HBr + H \rightleftharpoons Br + H_2 \tag{R2}$$

is so fast that it is effectively equilibrated in all but the very early stages of the flames. The equilibrium of this reaction is shifted to the right under flame conditions and HBr is converted to bromine atoms already in the preheating zone. For this reason, the inhibiting effect of HBr cannot be attributed to competition for atomic hydrogen between reaction (R2) and H + O_2 $\rightleftharpoons$ O+OH, as suggested in early studies of bromine inhibition. Similarly to the batch reactor experiments discussed above, HOBr is not predicted to be of significance for the inhibition.

Miller et al. [17] and Drake and Hastie [18] reported burning velocities of fuel-rich H_2/air flames with and without addition of HBr. Their flames were far from the flammability limit, characterized by much higher temperatures ($\approx$ 2000 K) and burning velocities than the flames of Day et al. Figure 11 compares measured and predicted laminar flame speeds for H_2/air/HBr mixtures as a function of the hydrogen bromine inlet mole fraction and inlet temperature. It is noteworthy that the results for the undoped flames at fuel/air

equivalence ratio of 1.75 and 2.0, respectively, of 274 cm s^{-1} and 261 cm s^{-1} are within the reported range of 260 to 285 cm s^{-1} ($1.75 \leq \phi \leq 2.0$) [142–145], even though they are slightly below the most recent values of 282-285 cm s^{-1} [144, 145].

Even though these flames are less sensitive to bromine inhibition than those of Day et al., the addition of 0.5% [18] and 3.1% [17] of HBr, respectively, is seen to reduce the H_2/air flame speed significantly. The model slightly overpredicts the flame speed, even in uninhibited conditions, but the effect of HBr addition is captured well.

Figure 12 shows sensitivity coefficients for the conditions of Fig. 11 and addition of 0, 3 and 6% HBr, respectively. In the absence of HBr, the predicted flame speed is sensitive to the key chain branching reaction,

$$H + O_2 \rightleftharpoons O + OH$$

and to the propagating steps,

$$OH + H_2 \rightleftharpoons H_2O + H$$

$$H + O_2(+M) \rightleftharpoons HO_2(+M)$$

$$HO_2 + H \rightleftharpoons OH + OH$$

All of these reactions exhibit positive sensitivity coefficients, even the H + O_2 (+M) reaction. The presence of bromine introduces a number of chain breaking steps that serve to reduce the flame speed,

$$H + Br + M \rightleftharpoons HBr + M \quad \text{(R1)}$$

$$Br + Br + M \rightleftharpoons Br_2 + M \quad \text{(R8)}$$

$$Br + HO_2 \rightleftharpoons HBr + O_2 \quad \text{(R7)}$$

Since the HO_2 radical now participates in a terminating reaction sequence involving (R7), the sensitivity coefficient for the H+O_2(+M) reaction shifts from a positive value at uninhibited conditions to a negative value at high HBr levels. The inhibiting steps are similar to those of the lower temperature flames of Day et al., except that also addition of atomic bromine recombination (R9) is now active. Similarly to the low-temperature flames, hydrogen bromide is largely consumed prior to the main reaction zone and HBr is not active in the chain-breaking cycle.

In Fig. 13 we use the updated chemical kinetic model to investigate Br_2/air mixtures as oxidizer for a flame containing 60% hydrogen, covering the full range of oxidizers from air to Br_2. For these flames, which are rich in the lighter component throughout, there are available experimental data at each end of the oxidizer range, but no data in the transition region with a mixture of air and bromine. The model predicts an interesting behavior. The burning velocity for 60% H_2 in air ($\phi = 3.57$) is almost 200 cm s^{-1} [142–144], while the 60% H_2/40% Br_2 mixture has a flame speed of about 30 cm s^{-1} [132]. Based on these observations, one could expect the flame speed to decrease monotonically as air was gradually replaced by bromine. However, addition of Br_2 even in minor quantities strongly inhibits the H_2/air flame and already at 3% Br_2, the flame speed falls below the value for the pure H_2/Br_2 flame (note the logarithmic scale). In the range 10-25% Br_2, the model predicts the flame speed to be close to the flammability limit of 5 cm s^{-1}, as defined by Bui-Pham et al. [146], with a minimum at 20% Br_2. Above 20% of Br_2, the burning velocity increases slowly with increasing bromine content, approaching the value of about 30 cm s^{-1} for the H_2/Br_2 flame.

Figure 14 shows sensitivity coefficients for selected H_2/air/Br_2 flames under conditions corresponding to Fig. 13. From these results and a corresponding flux analysis, we can explain the presence of the minimum in the flame speed according to the following. When Br_2 is fed in smaller amounts (<20%), it mainly reacts with atomic hydrogen,

$$Br_2 + H \rightarrow HBr + Br. \tag{R9}$$

This reaction serves to reduce the flame velocity, because Br_2 + H is much faster than H + O_2, promoting depletion of H atoms from the system. At low Br_2 concentrations, the Br atom produced in reaction (R9) can react with H_2 to form HBr and H (mechanism M1):

$$Br_2 + H \rightarrow HBr + Br \tag{R9}$$

$$Br + H_2 \rightarrow HBr + H \tag{R2b}$$

$$Br_2 + H_2 \rightarrow HBr + HBr$$

or recombine to form Br_2 (mechanism M2):

$$Br_2 + H \rightarrow HBr + Br \quad \text{(R9)}$$

$$Br + Br + M \rightarrow Br_2 + M \quad \text{(R8)}$$

$$Br + H \rightarrow HBr$$

In the M1 mechanism, Br reacts with H_2 to yield H (R2b), which partially supports the flame speed. Contrary to this, the M2 mechanism acts as a termination step. As $[Br_2]$ increases, the role of the M2 mechanism becomes progressively less important. In fact, under these conditions Br mainly reacts with H_2 because the thermodynamic equilibrium does not favor the recombination reaction (R8). At very high Br_2 concentrations, the recombination reaction (R8) acts as a decomposition step. In particular, for amounts of Br_2 larger than $\sim$25%, the M2 mechanism is progressively inhibited and this explains the increase in the flame speed observed in Fig. 13. It is important to notice that this increase is only a chemical effect and not a thermodynamic one. As a matter of fact, the addition of Br_2 monotonically decreases the flame temperature. This role of reaction (R8) on the flame speed is quite evident also from the sensitivity analysis in Fig. 14, which shows that for levels of Br_2 larger than $\sim$25%, this reaction serves to activate the system.

Effective flame inhibitors act through gas-phase catalytic cycles that lead to an effective radical recombination in the reaction zone. There is considerable evidence that a feature that is responsible for the ranking different kinetic inhibitors is the relative number of "catalytic" reaction cycles that remove active radicals [147, 148]. Bromine systems, along with other halogens, are the simplest because they contains the lowest variety of such radical removal reaction cycles, compared to organophosphorus and metal systems [148].

Conclusions

The high-temperature bromine chemistry was updated and the inhibition mechanisms involving HBr and Br_2 were re-examined. The thermochemistry

of the bromine species was obtained using the Active Thermochemical Tables (ATcT) approach. The accuracy of heats of formation for key species such as Br, HBr, HOBr and BrO was significantly improved, compared to earlier evaluations. Ab initio calculations were used to obtain rate coefficients for selected reactions of HBr and HOBr, i.e., HBr + HO_2, HOBr + HO_2, and HOBr + H. Based on the present work and results from literature, the hydrogen/bromine/oxygen reaction mechanism was updated. The resulting model was validated against selected experimental data from literature and used to analyze the effect of HBr and Br_2 on laminar, premixed hydrogen flames. Our work shows that hydrogen bromide and molecular bromine act differently as inhibitors in flames. For HBr, the reaction HBr + H $\rightleftharpoons$ H_2 + Br (R2) is rapidly equilibrated, depleting HBr in favor of atomic Br, which is the major bromine species throughout the reaction zone. The chain-breaking steps are then H + Br + M $\rightarrow$ HBr + M (R1), Br + HO_2 $\rightarrow$ HBr + O_2 (R7), and Br + Br + M $\rightarrow$ Br_2 + M (R8). In Br_2-doped flames, the reaction Br_2 + H $\rightleftharpoons$ HBr + Br (R9) is far from equilibration and serves to deplete H in the reaction zone by competing with H + O_2 $\rightarrow$ O + OH. The inhibition is augmented by recombination of Br (R8). If the inlet Br_2 mole fraction exceeds about 20%, reactions (R8) and (R2) are both reversed, now acting to promote chain branching and increase the flame speed. Cycles involving HOBr are not important for generation or removal of chain carriers in these flames.

Acknowledgements

To the authors' knowledge, this is the last paper co-authored by Graham Dixon-Lewis, whose death has deprived the combustion community of one of its finest scientists and most beloved colleagues. Graham had been working earlier on flame inhibition by bromine species (Refs. 30-32) and this topic still had his interest. After the PG plenary on the impact of trace species in combustion at the 31^{st} international symposium in Heidelberg in 2006 (Ref. 6), Graham took the initiative for the present work. Together with PG, he defined the scope of the work, chose the experiments to take into consideration, and particpated in the preliminary modeling. After his death, the group of collaborators was expanded to enhance the quality of the model

and resolve issues with the flame calculations. The work at Argonne National Laboratory was supported by the U.S. Department of Energy, Office of Basic Energy Sciences, Division of Chemical Sciences, Geosciences and Biosciences under Contract No. DE-AC02-06CH11357. Portions of this research are related to the effort of the Task Group of the International Union of Pure and Applied Chemistry, "Selected Free Radicals and Critical Intermediates: Thermodynamic Properties from Theory and Experiment" (IUPAC Project 2003-024-1-100). The UNT work was supported by the Robert A. Welch Foundation (Grant B-1174) and used computational facilities purchased with a National Science Foundation grant (CHE-0741936).

References

[1] F.C. Wofsy, M.B. McElroy, and Y.L. Yung. *Geophys. Res. Lett.* 2 (1975) 215.

[2] G. Soderstrom and S. Marklund. *Env. Sci. Technol.* 36 (2002) 1959.

[3] P. Vainikka, D. Bankiewicz, A. Frantsi, J. Silvennoinen, J. Hannula and. P. Yrjas, and M. Hupa. *Fuel*, 90 (2011) 2055.

[4] M.G. Bryukov, B. Dellinger, and V.D. Knyazev. *J. Phys. Chem. A* 110 (2006) 9169–9174.

[5] C.F. Cullis, A. Fish, and R.B. Ward. *Proc. Royal Soc. London* 276 (1963) 527–541.

[6] P. Glarborg. *Proc. Combust. Inst.* 31 (2007) 77–98.

[7] J.H. Burgoyne and G. Williams-Leir. *Proc. Roy. Soc. Lond.* 193 (1947) 525–539.

[8] J.H. Burgoyne and G. Williams-Leir. *Fuel Lond.* 27: (1948 118.

[9] E.H. Coleman. *Fuel Lond.* 30 (1951) 114.

[10] E.H. Coleman. *Fuel Lond.* 31 (1952) 445.

[11] M.G. Zabetakis. *Flammability characteristics of combustible gases and vapors.* Bulletin 627, US Bureau of Mines, 1965.

[12] H.F. Simmons and H.G. Wolfhard. *Trans. Faraday Soc.* 51 (1955) 1211.

[13] F.H. Garner, R. Long, A.J. Graham, and A. Badakshan. *Proc. Combust. Inst.* 6 (1957) 802–806.

[14] W.A. Rosser, H. Wise, and J. Miller. *Proc. Combust. Inst.* 7 (1959) 175–182.

[15] H.B. Palmer and D.J. Seery. *Combust. Flame* 4 (1960) 213–221.

[16] A. Levy, J.W. Droege, J.J. Tighe, and J.F. Foster. *Proc. Combust. Inst.* 8 (1962) 524–533.

[17] D.R. Miller, R.L. Evers, and G.B. Skinner. *Combust. Flame* 7 (1963) 137–142.

[18] M.C. Drake and J.W. Hastie. *Combust. Flame* 40 (1981) 201–211.

[19] C.H. Kim, O.C. Kwon, and G.M. Faeth. *J. Propul. Power* 18 (2002) 1059–1067.

[20] D.R. Blackmore, G. O'Donnell, and R.F. Simmons. *Proc. Combust. Inst.* 10 (1965) 303–310.

[21] D.R. Clark, R.F. Simmons, and D.A. Smith. *Trans. Farady Soc.* 66 (1970) 1423–1435.

[22] F. Battin-Leclerc, G.M. Come, and F. Baronnet. *Combust. Flame* 99 (1994) 644–652.

[23] F.F. Rust and W.E. Vaughn. *Ind. Eng. Chem.* 41 (1949) 2595–2597.

[24] E.R. Bell, F.H. Dickey, J.H. Raley, F.F. Rust, and W.E. Vaughn. *Ind. Eng. Chem.* 41 (1949) 2597–2604.

[25] E.R. Allen and C.F.H. Tipper. *Proc. Roy. Soc. Lond.* A258 (1960) 251.

[26] A. Hardager, G. Skirrow, and C.F.H. Tipper. *Combust. Flame* 7 (1963) 100–1012.

[27] A. Hardager, G. Skirrow, and C.F.H. Tipper. *Combust. Flame* 9 (1965) 53–61.

[28] P. Hurst, G. Skirrow, and C.F.H. Tipper. *Proc. Roy. Soc. London* 268 (1962) 405–423.

[29] L.A. Lovachev, V.T. Gontkovskaya, and N.I. Ozerkovskaya. *Combust. Sci. Technol.* 17 (1977) 143–151.

[30] M.J. Day, D.V. Stamp, K. Thompson, and G. Dixon-Lewis. *Proc. Combust. Inst.* 13 (1971) 705–712.

[31] G. Dixon-Lewis and R.J. Simpson. *Proc. Combust. Inst.* 16 (1977) 1111–1119.

[32] G. Dixon-Lewis. *Combust. Flame* 36 (1979) 1–14.

[33] C.K. Westbrook. *Combust. Sci Technol.* 23 (1980) 191–202.

[34] C.K. Westbrook. *Proc. Combust. Inst.* 19 (1982) 127–141.

[35] B. Walravens, F. Battin-Leclerc, G.M. Come, and F. Baronnet. *Combust. Flame* 103 (1995) 399–342.

[36] V. Babushok, T. Noto, D.R.F. Burgess, A. Hamins, and W. Tsang. *Combust. Flame* 107 (1996) 351–367.

[37] T. Noto, V. Babushok, A. Hamins, and W. Tsang. *Combust. Flame* 112 (1998) 147–160.

[38] B.A. Williams and J.W. Fleming. *Proc. Combust. Inst.* 29 (2002) 345–351.

[39] K. Seshadri. *Combust. Sci. Technol.* 177 (2005) 871–906.

[40] C.F. Cullis, A. Fish, and R.B. Ward. *Combust. Flame* 7 (1963) 303–304.

[41] B. Ruscic, R.E. Pinzon, M.L. Morton, G. von Laszewski, S. Bittner, S. G. Nijsure, K. A. Amin, M. Minkoff, and A. F. Wagner. *J. Phys. Chem. A* 108 (2004) 9979–9997.

[42] B. Ruscic, R. E. Pinzon, G. von Laszewski, D. Kodeboyina, A. Burcat, D. Leahy, D. Montoya, and A. F. Wagner. *J. Phys. Conf. Ser.* 16 (2005) 561–570.

[43] B. Ruscic, R. E. Pinzon, M. L. Morton, N. K. Srinivasan, M.-C. Su, J. W. Sutherland, and J. V. Michael. *J. Phys. Chem. A* 110 (2006) 6592–6601.

[44] S. L. Widicus Weaver, D. E. Woon, B. Ruscic, and B. J. McCall. *Astrophys. J.* 697 (2009) 601–609.

[45] W. R. Stevens, B. Ruscic, and T. Baer. *J. Phys. Chem. A* 114 (2010) 13134–13145.

[46] B. Ruscic, J. V. Michael, P. C. Redfern, L. A. Curtiss, and K. Raghavachari. *J. Phys. Chem. A* 102 (1998) 10889–10899.

[47] B. Ruscic, M. Litorja, and R. L. Asher. *J. Phys. Chem. A* 103 (1999) 8625–8633.

[48] R. Sivaramakrishnan, M.-C. Su, J. V. Michael, S. J. Klippenstein, L. B. Harding, and B. Ruscic. *J. Phys. Chem. A* 114 (2010) 9425–9439.

[49] E. Goos, A. Burcat, and B. Ruscic. Ideal gas thermochemical database with updates from active thermochemical tables (<ftp://ftp.technion.-ac.il/pub/supported/aetdd/thermodynamics> mirrored at <http://-garfield.chem.elte.hu/burcat/burcat.html>.

[50] A. Burcat and B. Ruscic. Third millenium ideal gas and condensed phase thermochemical database for combustion with updates from active chemical tables. Technical Report Report TAE 960 and ANL-05/20, Technion-IIT, Haifa, and Argonne National Laboratory, Argonne, Illinois, 2005.

[51] J. D. Cox, D. D. Wagman, and V. A. Medvedev. *CODATA Key Values for Thermodynamics*. Hemisphere, New York, 1989.

[52] S. Gerstenkorn and P. Luc. *J. Phys. (France)* 50 (1989) 1417–1432.

[53] M. Penno, A. Holzwarth, and K.-M. Weitzel. *J. Phys. Chem. A* 102 (1998) 1927–1934.

[54] J. R. Lacher, A. Kianpour, F. Oetting, and J. D. Park. *Trans. Faraday Soc.* 52 (1956) 1500–1508.

[55] J. R. Lacher, L. Casali, and J. D. Park. *J. Phys. Chem.* 60 (1956) 608–610.

[56] G. Jones and S. Baeckstrom. *J. Am. Chem. Soc.* 56 (1934) 1524–1528.

[57] H. von Wartenberg and G. Z. Klinkott. *Z. Anorg. Allgem. Chem.* 193 (1930) 409–419.

[58] H. von Wartenberg. *Z. Anorg. Allgem. Chem.* 200 (1931) 235–236.

[59] V. B. Parker. *Thermal Properties of Aqueous Uni-Univalent Electrolytes*. NSRDS-NBS 2, US Gov. Printing Office, Washington, DC, 1965.

[60] W. A. Roth and A. Z. Bertram. *Z. Elektrochem.* 63 (1937) 376–378.

[61] J. Thomsen. *Thermochemishe Untersuchungen.* J.A. Barth, Leipzig, 1882-1886.

[62] R. Haase, H. Naas, and H. Thumm. *Z. Phys. Chem. (Frankfurt)* 37 (1963) 210–229.

[63] C. E. Vanderzee and J. D. Nutter. *J. Phys. Chem.* 67 (1963) 2521–2523.

[64] S. Sunner and S. Thoren. *Acta Chem. Scand.* 18 (1964) 1528–1532.

[65] R. A. Durie and D. A. Ramsay. *Can. J. Phys.* 36 (1958) 35–53.

[66] M. Barnett, E. A. Cohen, and D. A. Ramsay. *Can. J. Phys.* 59 (1981) 1908–1916.

[67] D. M. Wilmouth, T. F. Hanisco, N. M. Donahue, and J. G. Anderson. *J. Phys. Chem. A* 103 (1999) 8935–8945.

[68] O. C. Fleischmann, M. Hartmann, J. P. Burrows, and J. Orphal. *J. Photochem. Photobiol. A* 168 (2004) 117–132.

[69] H. Kim, K. S. Dooley, E. R. Johnson, and S. W. North. *J. Chem. Phys.* 124 (2006) 134304/1–8.

[70] P. Zou, H. Kim, and S. W. North. *J. Chem. Phys.* 116 (2002) 4176–4183.

[71] B. J. Drouin, C. E. Miller, H. S. P. Muller, and E. A. Cohen. *J. Mol. Spectrosc.* 205 (2001) 128–138.

[72] V. Ramakrishna and B. J. Duke. *J. Chem. Phys.* 118 (2003) 6137–6143.

[73] D. Feller, K. A. Peterson, and D. A. Dixon. *J. Chem. Phys.* 129 (2008) 204105/1–32.

[74] D. J. Grant, E. B. Garner III, M. H. Matus, M. T. Nguyen andK. A. Peterson, J. S. Francisco, and D. A. Dixon. *J. Phys. Chem. A* 114 (2010) 4254–4265.

[75] K. A. Peterson, B. C. Shepler, D. Figgen, and H. Stoll. *J. Phys. Chem. A* 110 (2006) 13877–13883.

[76] B. C. Shepler and K. A. Peterson. *J. Phys. Chem. A* 110 (2006) 12321–12329.

[77] S. Yockel, B. Mintz, and A. K. Wilson. *J. Chem. Phys.* 121 (2004) 60–77.

[78] P. Hassanzadeh and K. K. Irikura. *J. Phys. Chem. A* 101 (1997) 1580–1587.

[79] Ed. M. W. Chase, Jr. *NIST-JANAF Thermochemical Tables*. 4th ed., J. Phys. Chem. Ref. Data, Monogr. 9, 1998.

[80] L. V. Gurvich, I. V. Veyts, and C. B. Alcock. *Thermodynamic Properties of Individual Substances*. Vol. 1, Parts 1 and 2, Hemisphere, New York, 1989.

[81] B. Ruscic and J. Berkowitz. *J. Chem. Phys.* 101 (1994) 7795–7803.

[82] B. Ruscic, A. F. Wagner, L. B. Harding, R. L. Asher, D. Feller, D. A. Dixon, K. A. Peterson, Y. Song, X. Qian, C.-Y. Ng, J. Liu, W. Chen, and D. W. Schwenke. *J. Phys. Chem. A* 106 (2002) 2727–2747.

[83] B. Ruscic, D. Feller, D. A. Dixon, K. A. Peterson, L. B. Harding, R. L. Asher, and A. F. Wagner. *J. Phys. Chem. A* 105 (2001) 1–4.

[84] B. Ruscic and J. Berkowitz. *J. Chem. Phys.* 101 (1994) 9215–9218.

[85] P. S. Monks, F. L. Nesbitt, M. Scanlon, and L. J. Stief. *J. Phys. Chem.* 97 (1993) 11699–11705.

[86] A. Kukui, U. Kirchner, T. Benter, and R. N. Schindler. *Ber. Bunsenges. Phys. Chem.* 100 (1996) 455–461.

[87] L. M. Loewenstein and J. G. Anderson. *J. Phys. Chem.* 88 (1984) 6277–6286.

[88] M. Lock, R. J. Barnes, and A. Sinha. *J. Phys. Chem.* 100 (1996) 7972–7980.

[89] T. J. Lee. *J. Phys. Chem.* 99 (1995) 15074–15080.

[90] M. N. Glukhovtsev, A. Pross, and L. Radom. *J. Phys. Chem.* 100 (1996) 3498–3503.

[91] Y. Ren, J. L. Wolk, and S. Hoz. *Int. J. Mass Spectrom.* 220 (2002) 1–10.

[92] P.A. Denis. *J. Phys. Chem. A* 110 (2006) 5887–5892.

[93] J. J. Orlando and J. B. Burkholder. *J. Phys. Chem.* 99 (1995) 1143–1150.

[94] Jr. R. P. Thorn, P. S. Monks, L. J. Stief, S.-C. Kuo, Z. Zhang, and R. B. Klemm. *J. Phys. Chem.* 100 (1996) 12199–12203.

[95] F. Grein. *J. Phys. Chem. A* 114 (2010) 6157–6163.

[96] M. Alcami and I. L. Cooper. *J. Chem. Phys.* 108 (1998) 9414–9424.

[97] R. Vetter, Th. Ritschel, L. Zulicke, and K. A. Peterson. *J. Phys. Chem. A*, 107 (2003) 1405–1412.

[98] K. Suma, Y. Sumiyoshi, and Y. Endo. *J. Chem. Phys.* 123 (2005) 024312/1–6.

[99] M.J. Frisch, G.W. Trucks, H.B. Schlegel, G.E. Scuseria, M.A. Robb, J.R. Cheeseman, G. Scalmani, V. Barone, B. Mennucci, G.A. Petersson, H. Nakatsuji, M. Caricato, X. Li, H.P. Hratchian, A.F. Izmaylov, J. Bloino, G. Zheng, J.L. Sonnenberg, M. Hada, M. Ehara, K. Toyota, R. Fukuda, J. Hasegawa, M. Ishida, T. Nakajima, Y. Honda, O. Kitao, H. Nakai, T. Vreven, J. Montgomery, J.E. Peralta, F. Ogliaro, M. Bearpark, J.J. Heyd, E. Brothers, K.N. Kudin, V.N. Staroverov, R. Kobayashi, J. Normand, K. Raghavachari, A. Rendell, J.C. Burant, S.S. Iyengar, J. Tomasi, M. Cossi, M. Rega, M. Klene, J.E. Knox, J.B. Cross, V. Bakken, C. Adamo, J. Jaramillo, R.E. Gomperts, O. Stratmann, A.J. Yazyev, R. Austin, C. Cammi, J.W. Pomelli, R. Ochterski, R.L. Martin, K. Morokuma, V.G. Zakrzewski, G.A. Voth, P. Salvador, J.J. Dannenberg, S. Dapprich, A.D. Daniels, O. Farkas, J.B. Foresman, J.V. Ortiz, J. Cioslowski, and D.J. Fox. *Gaussian 09*. Gaussian, Wallingford, CT, 2009.

[100] H.-J. Werner, P.J. Knowles, R. Lindh, F.R. Manby, M. Schutz, P. Celani, T. Korona, A. Mitrushenkov, G. Rauhut, T.B. Adler, R.D. Amos, A. Bernhardsson, A. Berning, D.L. Cooper, M.J.O. Deegan, A.J. Dobbyn, F. Eckert, E. Goll, C. Hampel, G. Hetzer, T. Hrenar,

G. Knizia, C. Köppl, Y. Liu, A.W. Lloyd, R.A. Mata, A.J. May, S.J. McNicholas, W. Meyer, M.E. Mura, A. Nicklass, P. Palmieri, K Pflüger, R. Pitzer, M. Reiher, U. Schumann, H. Stoll, A.J. Stone, R. Tarroni, T. Thorsteinsson, M. Wang, and A. Wolf. *Molpro Quantum Chemistry Package*. 2009.

[101] A. Halkier, T. Helgaker, P. Jorgensen, W. Klopper, H. Koch, J. Olsen, and A.K. Wilson. *Chem. Phys. Lett.* 286 (1998) 243.

[102] A. Mellouki, R.K. Talukdar, and C.J. Howard. *J. Geophys. Res.* 99 (1994) 22949–22954.

[103] D.W. Toohey, W.H. Brune, and J.G. Anderson. *J. Phys. Chem.* 91 (1987) 1215.

[104] S.P. Heneghan and S.W. Benson. *Int. J. Chem. Kinet.* 15 (1983) 1311–1319.

[105] S. Antonik and M. Lucquin. *Bul. Soc. Chim. France* 8-9 (1970) 2861.

[106] V.F. Kochubei and F.B. Moin. *Dokl. Akad. Naut. SSSR* 219 (1974) 141.

[107] L.G.S. Shum and S.W. Benson. *Int. J. Chem. Kinet.* 15 (1983) 341–380.

[108] M.-T. Leu. *Chem. Phys. Lett.* 69 (1980) 37–39.

[109] J. Posey, J. Sherwell, and M. Kaufman. *Chem. Phys. Lett.* 77 (1981) 476.

[110] J. Troe. *J. Phys. Chem.* 83 (1979) 114.

[111] L. Wang, J. Liu, Z. Li, X. Huang, and C. Sun. *J. Phys. Chem. A* 107 (2003) 4921.

[112] Z.F. Xu and M.C. Lin. *J. Phys. Chem. A* 113 (2009) 8811.

[113] L. Li, Z.W. Zhao, A. Kazakov, and F.L. Dryer. *Int. J. Chem. Kinet.* 36 (2004) 566–575.

[114] M. O'Conaire, H.J. Curran, J.M. Simmie, W.J. Pitz, and C.K. Westbrook. *Int. J. Chem. Kinet.* 36 (2004) 603–622.

[115] S.G. Davis, A.V. Joshi, H. Wang, and F. Egolfopoulos. *Proc. Combust. Inst.* 30 (2005) 1283–1292.

[116] A. Frassoldati, T. Faravelli, and E. Ranzi. *Int. J. Hydrogen Energy* 31 (2006) 2310–2328.

[117] A.A. Konnov. *Combust. Flame* 152 (2008) 507–528.

[118] C.L. Rasmussen, J. Hansen, P. Marshall, and P. Glarborg. *Int. J. Chem. Kinet.* 40 (2008) 454–480.

[119] M.P. Burke, M. Chaos, F.L. Dryer, and Y.G. Ju. *Combust. Flame* 157 (2010) 618–631.

[120] S.R. Sellevåg, Y. Georgievskii, and J. A. Miller. *J. Phys. Chem. A* 112 (2008) 5085–5095.

[121] D.L. Baulch, J. Duxbury, S.J. Grant, and D.C. Montague. *J. Phys. Chem. Ref. Data* 10, supplement, 1981.

[122] P.W. Seakins and M.J. Pilling. *J. Phys. Chem.* 95 (1991) 9878–9881.

[123] W.B. DeMore, S.P. Sander, D.M. Golden, R.F. Hampson, M.J. Kurylo, C.J. Howard, A.R. Ravishankara, C.E. Kolb, and M.J. Molina. Chemical kinetics and photochemical data for use in stratospheric modeling. Evaluation number 12. Technical Report 97-4, JPL Publication, 1997.

[124] R. Atkinson, D.L. Baulch, R.A. Cox, J.N. Crowley, R.F. Hampson Jr., R.G. Hynes, M.E. Jenkin, M.J. Rossi, and J. Troe. *Atmos. Chem. Phys.* 7 (2007) 981–1191.

[125] J.C. Hansen, Y. Li, Z. Li, and J.S. Francisco. *Chem. Phys. Lett.* 314 (1999) 341–346.

[126] M.H. Harwood, D.M. Rowley, R.A. Cox, and R.L. Jones. *J. Phys. Chem. A* 102 (1998) 1790–1802.

[127] L. Wang, J.Y. Liu, Z.S. Li, and C.C. Sun. *J. Comput. Chem.* 25 (2004) 558–564.

[128] G. Laverdet, G. Le Bras, A. Mellouki, and G. Poulet. *Chem. Phys. Lett.* 172 (1990) 430.

[129] Y. Bedjanian, V. Riffault, G. Le Bras, and G. Poulet. *J. Phys. Chem. A* 105 (2001) 573–578.

[130] R. Sumathi and S.D. Peyerimho. *Phys. Chem. Chem. Phys.* 1 (1999) 3973–3979.

[131] V.I. Jaramillo, S. Gougeon, S.D. le Picard, A. Casano, M.A. Smith, and B.R. Rowe. *Int. J. Chem. Kinet.* 34 (2002) 339–344.

[132] S.D. Cooley, J.A. Lasater, and R.C. Anderson. *J. Am. Chem. Soc.* 74 (1952) 739–743.

[133] S.D. Cooley and R.C. Anderson. *Ind. Eng. Chem.* 44 (1952) 1402–1406.

[134] S.D. Cooley and R.C. Anderson. *J. Am. Chem. Soc.* 77 (1955) 235–237.

[135] M.C. Huffstutler, J.A. Rode, and R.C. Anderson. *J. Am. Chem. Soc.* 77 (1955) 809–810.

[136] G.C. Frazier, R.M. Fristrom, and J.F. Wehner. *AIChE J.* 9 (1965) 689–693.

[137] D. Britton and N. Davidson. *J. Chem. Phys.* 23 (1955) 2461.

[138] M.N. Plooster and D. Garvin. *J. A. Chem. Soc.* 78 (1956) 6003.

[139] D. Britton and R.M. Cole. *J. Phys. Chem.* 65 (1961) 1302–1308.

[140] A. Levy. *J. Phys. Chem.* 62 (1958) 570–574.

[141] Z. Hong, D. F. Davidson, and R. K. Hanson. *Combust. Flame* 158 (2011) 633–644.

[142] D.R. Dowdy, D.B. Smith, and S.C. Taylor. *Proc. Combust. Inst.* 23 (1990) 325.

[143] K.T. Aung, M.I. Hassan, and G.M. Faeth. *Combust. Flame* 109 (1997) 1.

[144] S.D. Tse, D.L. Zhu, and C.K. Law. *Proc. Combust. Inst.* 28 (2000) 1793.

[145] O.C. Kwon and G.M. Faeth. *Combust. Flame* 124 (2001) 590.

[146] M.N. Bui-Pham, A.E. Lutz, J.A. Miller, M. Desjardin, D.M. O'Shaughnessey, and R.J. Zondlak. *Combust. Sci. Technol.* 109 (1995) 71.

[147] V.I. Babushok and W. Tsang. *Combust. Flame* 123 (2000) 488–506.

[148] V. Babushok and W. Tsang. *Prog. Energy Combust. Sci.* 34 (2008) 288–329.

Table 1: Thermodynamic properties for selected bromine species [49]. Units are kJ mol^{-1} and J mol^{-1} K^{-1}.

Species	$H_{f,298}$	S_{298}	$C_{p,300}$	$C_{p,400}$	$C_{p,500}$	$C_{p,600}$	$C_{p,800}$	$C_{p,1000}$	$C_{p,1500}$	$C_{p,2000}$
Br	111.85±0.06	175.02	20.79	20.79	20.80	20.83	21.03	21.37	22.26	22.71
Br_2	30.88±0.11	245.47	36.06	36.73	37.08	37.31	37.59	37.79	38.26	39.09
HBr	-35.85±0.15	198.70	29.14	29.22	29.45	29.87	31.06	32.33	34.76	36.22
HOBr	-61.78±0.54	247.78	38.36	41.13	43.23	44.82	47.14	48.92	52.16	54.15
BrO	123.61±0.29	232.90	34.14	37.06	38.74	39.56	39.94	39.77	39.26	39.08
BrOO	110.17±3.89	283.39	46.58	48.84	50.61	52.02	54.03	55.26	56.75	57.36
OBrO	158.18±2.68	270.66	45.24	49.11	51.63	53.31	55.24	56.24	57.31	57.89
BrBrO	164.90±2.14	302.17	51.30	53.48	54.83	55.72	56.97	58.56	67.20	76.09
BrOBr	104.61±1.18	290.49	50.05	52.98	54.62	55.62	56.69	57.33	67.35	119.13

Table 2: Coupled cluster energies and density functional zero-point vibrational energies (scaled by 0.967).

Species	CCSD(T)/ cc-pVTZ-PP (au)	CCSD(T)/ cc-pVQZ-PP (au)	CBS extrapolation (au)	scaled zero-point energy (au)	relative 0 K enthalpy (kJ mol^{-1})
HO_2	-150.71254	-150.75977	-150.79423	0.01361	
HBr	-416.29302	-416.31381	-416.32897	0.00573	
TS5(HBr+HO_2)	-566.98865	-567.05705	-567.10697	0.01984	44.0
H	-0.49981	-0.49995	-0.50004	0.00000	
HOBr	-491.36733	-491.41332	-491.44687	0.01221	
TS20(H+HOBr)	-491.84786	-491.89414	-491.92792	0.00944	42.7
TS25(HOBr+HO_2)	-642.05062	-642.14514	-642.21411	0.02406	66.2

Table 3: Rate coefficients for reactions in the Br/H/O subset of the reaction mechanism. The rate constants are expressed in terms of a modified Arrhenius, K = A T^n exp(-E_a/(RT)). Units are cm, mol, s, J.

		A	n	E_a	Source
1.	$H + Br + M \rightleftharpoons HBr + M$[a]	1.9E21	-1.87	0	[121]
2.	$HBr + H \rightleftharpoons Br + H_2$	1.3E10	1.05	682	[122]
3.	$HBr + O \rightleftharpoons Br + OH$	3.5E12	0.00	12481	[123]
4.	$HBr + OH \rightleftharpoons Br + H_2O$	4.0E12	0.00	-1290	[124]
5.	$HBr + HO_2 \rightleftharpoons Br + H_2O_2$	4.2E02	2.93	32123	pw (500-2000 K)
6.	$HBr + BrO \rightleftharpoons HOBr + Br$	1.3E10	0.00	15070	[125]
7.	$Br + HO_2 \rightleftharpoons HBr + O_2$	8.6E09	1.00	1960	see text
8.	$Br + Br + M \rightleftharpoons Br_2 + M$[b]	1.5E14	0.00	-7118	[121]
	$Br + Br + Br_2 \rightleftharpoons Br_2 + Br_2$	1.1E15	0.00	-4383	[121]
9.	$Br_2 + H \rightleftharpoons HBr + Br$	4.6E07	2.05	-7553	[122]
10.	$Br_2 + O \rightleftharpoons Br + BrO$	3.1E11	0.00	-8211	[126]
11.	$Br_2 + OH \rightleftharpoons HOBr + Br$	1.1E15	-0.66	0	[4]
12.	$BrO + H \rightleftharpoons Br + OH$	3.0E13	0.00	0	[36] est
13.	$BrO + H \rightleftharpoons HBr + O$	1.0E12	0.00	0	[36] est
14.	$BrO + O \rightleftharpoons Br + O_2$	1.1E13	0.00	-1913	[124]
15.	$BrO + OH \rightleftharpoons Br + HO_2$	1.1E13	0.00	-2081	[124]
16.	$BrO + HO_2 \rightleftharpoons HOBr + O_2$	2.7E12	0.00	-4162	[124]
17.	$BrO + BrO \rightleftharpoons Br + Br + O_2$	1.6E12	0.00	0	[124]
18.	$BrO + BrO \rightleftharpoons Br_2 + O_2$	1.7E10	0.00	-6992	[124]
19.	$HOBr(+M) \rightleftharpoons Br + OH(+M)$	1.0E15	0.00	203900	est
	Low pressure limit	1.3E22	-1.52	213960	pw (700-2000 K)
20.	$HOBr + H \rightleftharpoons BrO + H_2$	2.0E07	1.91	33546	pw (298-2000 K)
21.	$HOBr + H \rightleftharpoons HBr + OH$	3.0E13	0.00	0	est, see text
22.	$HOBr + H \rightleftharpoons Br + H_2O$	3.0E13	0.00	0	est, see text
23.	$HOBr + O \rightleftharpoons BrO + OH$	7.2E13	0.00	3576	[124]
24.	$HOBr + OH \rightleftharpoons BrO + H_2O$	1.9E02	3.12	-5234	[127]
25.	$HOBr + HO_2 \rightleftharpoons BrO + H_2O_2$	1.0E00	3.55	54808	pw (500-2000 K)
26.	$Br + O_2 + M \rightleftharpoons BrOO + M$	2.3E24	-3.90	0	est, c
27.	$BrOO + H \rightleftharpoons BrO + OH$	3.0E13	0.00	0	est, c
28.	$BrOO + O \rightleftharpoons BrO + O_2$	3.0E13	0.00	0	est, c
29.	$BrOO + OH \rightleftharpoons BrO + HO_2$	2.0E12	0.00	0	est
30.	$BrOO + Br \rightleftharpoons Br_2 + O_2$	1.0E14	0.00	0	est, c

a: Third body efficiencies: HBr=2.7, H_2O=5

b: Third body efficiencies: N_2=1.25, H_2O=5.4, Br_2=0

c: Estimated by analogy to the corresponding chlorine reaction

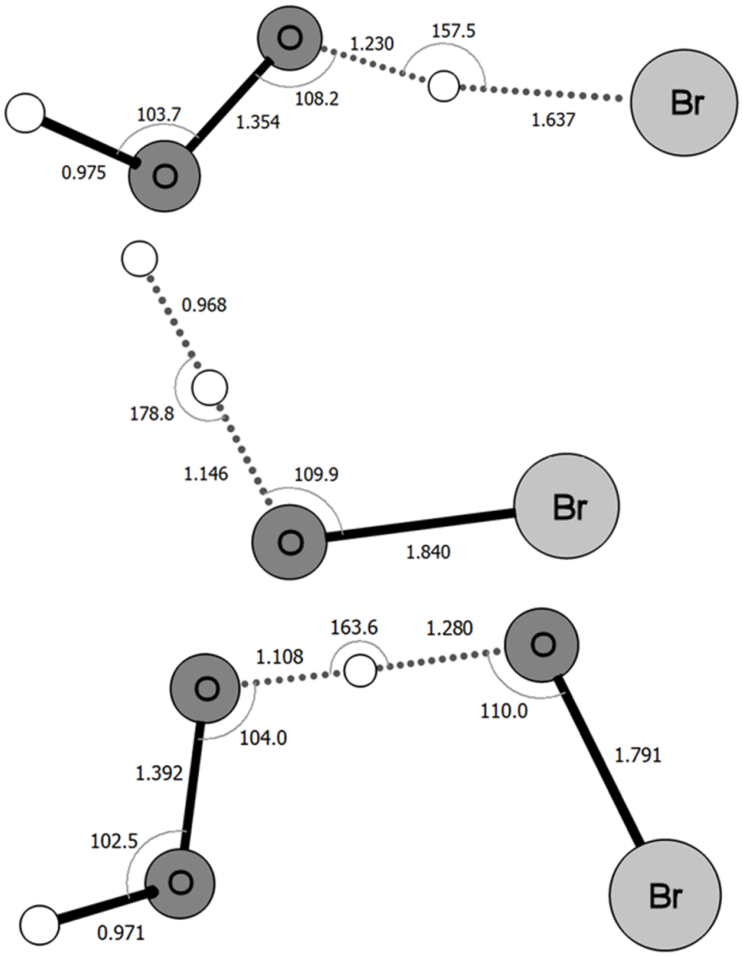

Figure 1: Transition state geometries (bond lengths in 10^{-10} m and angles in degrees) and frequencies (in cm^{-1}, scaled by 0.967) computed at the B3LYP/6-311+G(d,p) level of theory for three reactions. From top to bottom: 1) TS5 for HBr + $HO_2 \rightarrow$ Br + H_2O_2. The dihedral angles HOOH and OOHBr are 132.3^o and -100.5^o, respectively. The frequencies are 1388 i, 142, 291, 363, 868, 1040, 1068, 1386, 3550. 2) TS20 for H + HOBr $\rightarrow$ H_2 + BrO The dihedral angle HHOBr is 180.0^o. The frequencies are 1478 i, 344, 591, 642, 1089, 1478. 3) TS25 for HOBr + $HO_2 \rightarrow$ BrO + H_2O_2. The dihedral angles HOOH, OOHO and OHOBr are 126.8^o, -84.5^o and 79.4^o, respectively. The frequencies are 1194 i, 72, 81, 283, 332, 515, 674, 997, 1120, 1338, 1553, 3595.

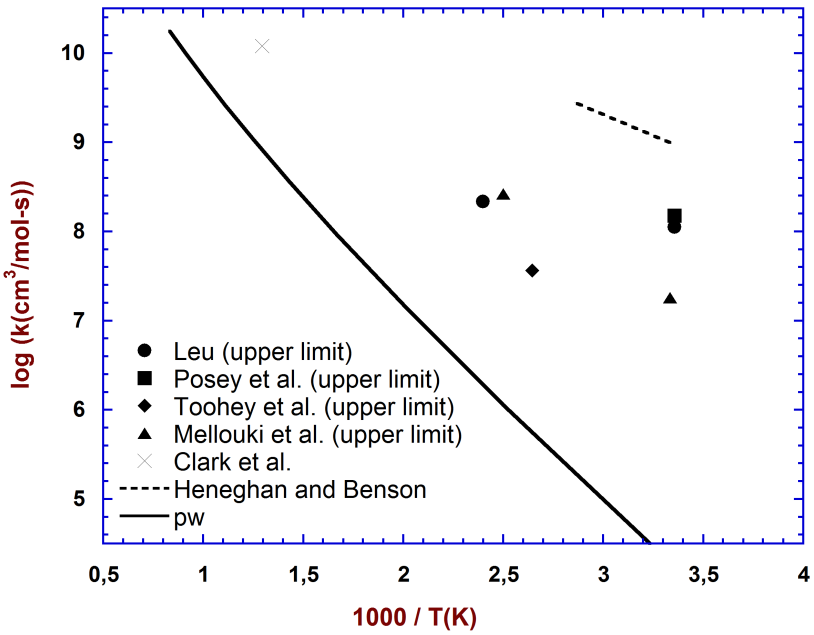

Figure 2: Arrhenius plot for the reaction HBr + $HO_2 \rightleftharpoons$ Br + H_2O_2 (R5). The symbols denote experiments results: Leu [108], Posey et al. [109], Toohey et al. [103], Mellouki et al. [102], and Heneghan and Benson [104]. The rate constants of Leu, Posey et al., Toohey et al., and Heneghan and Benson were derived from their values for the reverse reaction, using using the equilibrium constant. The solid line denotes the rate constant used in the present work.

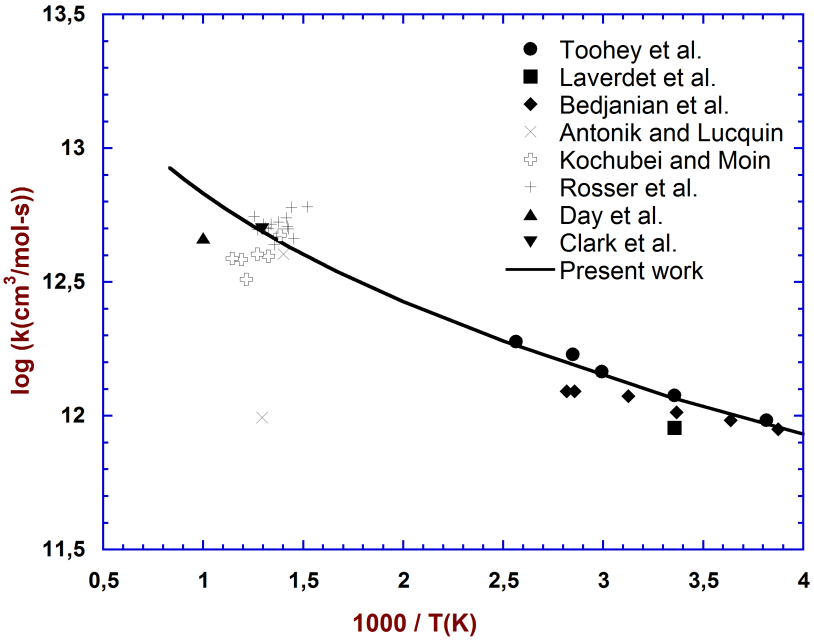

Figure 3: Arrhenius plot for the reaction Br + HO_2 $\rightleftharpoons$ HBr + O_2 (R7). The symbols denote experiments results: Toohey et al. [103], Laverdet et al. [128], and Bedjanian et al. [129], Antonik and Lucquin [105], Kochubei and Moin [106], Rosser et al. [14], Day et al. [30], and Clark et al. [21]. The solid line denotes the rate constant used in the present work.

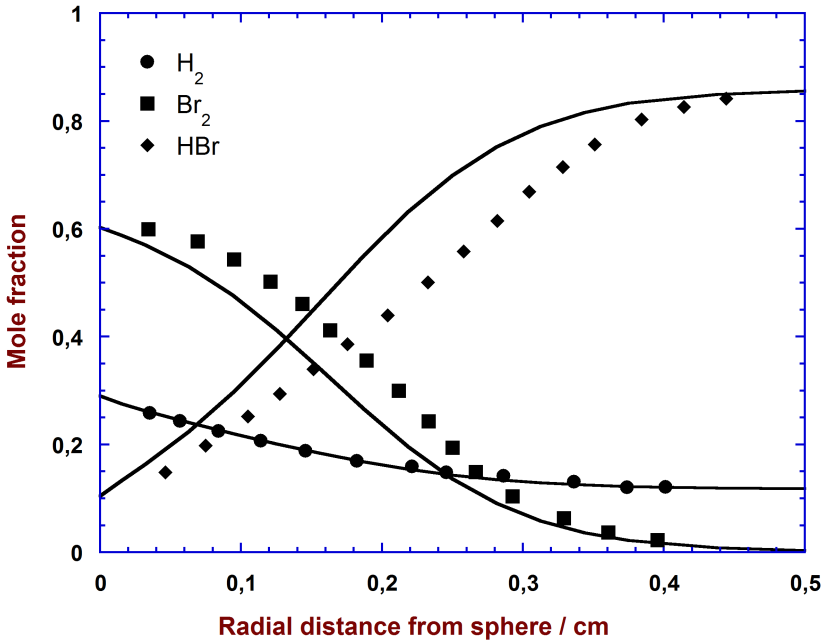

Figure 4: Comparison between experimental [136] and predicted structure for a spherical, low-pressure H_2/Br_2 flame. The flame had an initial content of 44.2% bromine, a pressure of 0.117 atm, and a corrected burning velocity at 298 K of 23.4 cm/s. The modeling predictions are conducted using the measured temperature profile [136].

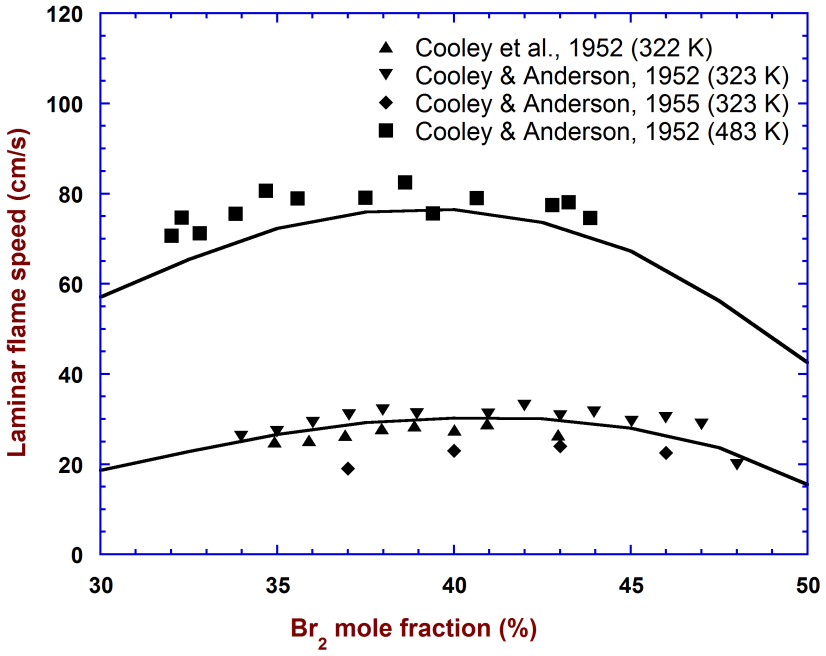

Figure 5: Comparison between measured and predicted laminar flame speeds for H_2/Br_2 mixtures as a function of the bromine inlet mole fraction and inlet temperature. Symbols represent measured values, while the curves represent predictions with the current mechanism. The experimental data are drawn from Cooley et al., 1952 [132], Cooley and Anderson, 1952 [133], and Cooley and Anderson, 1955 [134].

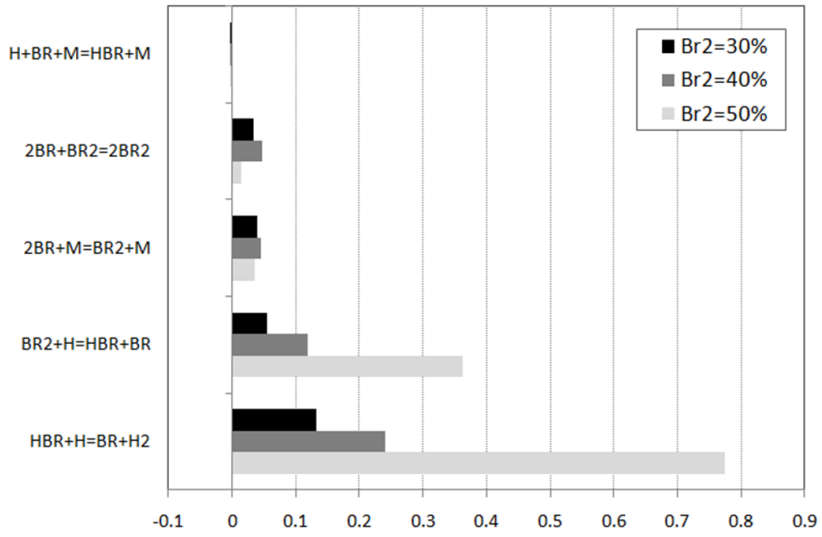

Figure 6: Linear sensitivity coefficients for the predicted laminar flame speed for H_2/Br_2 mixtures. Conditions similar to those of Fig. 5 (323 K).

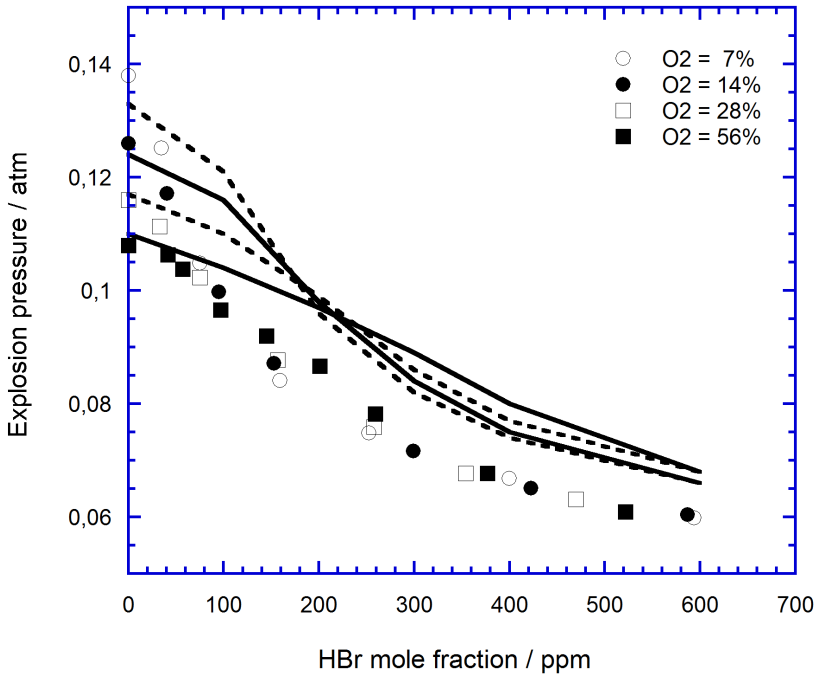

Figure 7: Comparison between experimental data (symbols) [21] and modeling predictions (lines) for the effect of HBr on the second pressure limit of explosion of H_2/O_2 mixtures in a batch reactor at 773 K. X_{HBr} denotes the mole fraction of HBr. Solid lines correspond to closed symbols while dashed lines correspond to open symbols. Inlet composition: 28% H_2, 7-56% O_2, 0-600 ppm HBr; balance N_2. The H_2/O_2/HBr was initially held at a pressure greater than the second limit; then gases were withdrawn until explosion occurs. In the modeling of these experiments, the low pressure limit rate constant for $H+O_2+N_2$ was lowered by 10%. The onset of rapid reaction within a reactor residence time of 10 s (arbitrarily chosen) constituted the criterion for explosion.

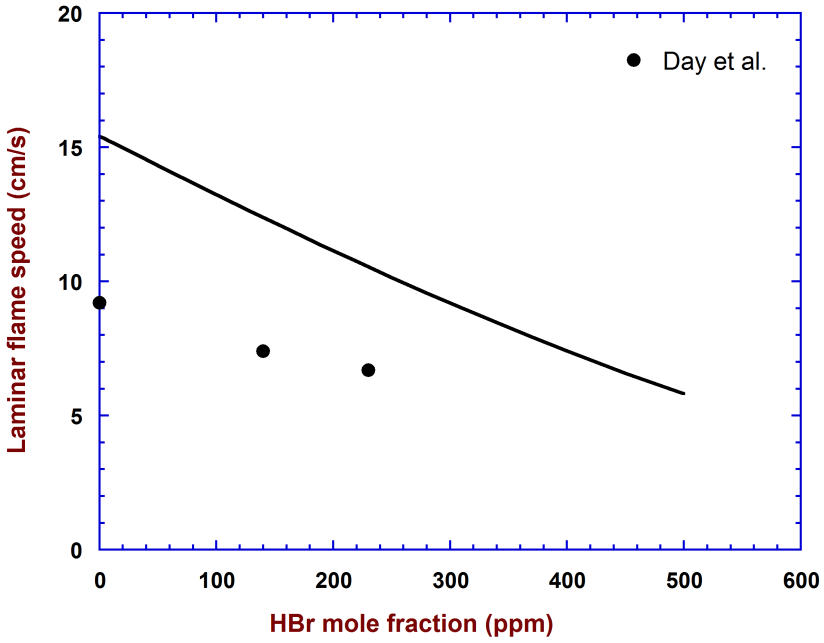

Figure 8: Comparison between measured [30] and predicted laminar flame speeds for $H_2/O_2/N_2$/HBr mixtures at 336 K as a function of the hydrogen bromine inlet mole fraction. Symbols represent measured values, while the solid line represents predictions with the current mechanism. The composition of the inlet gas was 18.8% H_2, 4.6% O_2 and 76.6% N_2, with varying amounts of HBr.

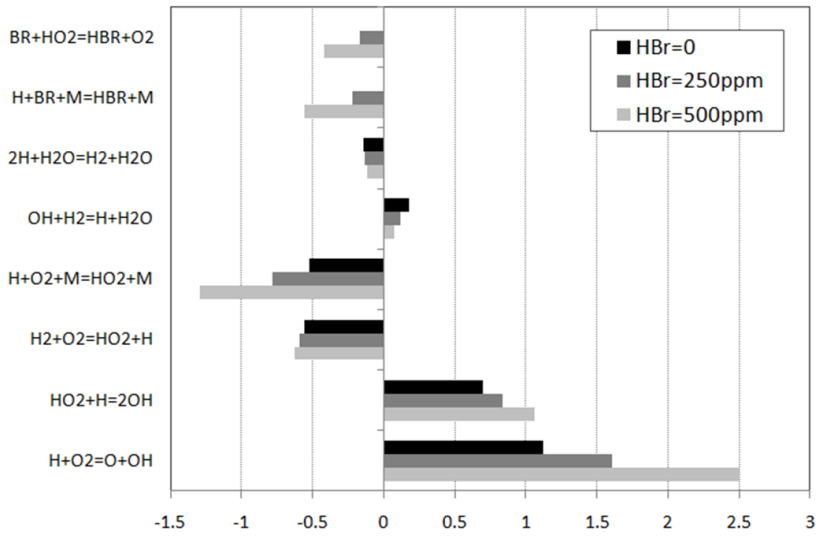

Figure 9: Linear sensitivity coefficients for the predicted laminar flame speed for H_2/air/HBr mixtures. Conditions similar to those of Fig. 8.

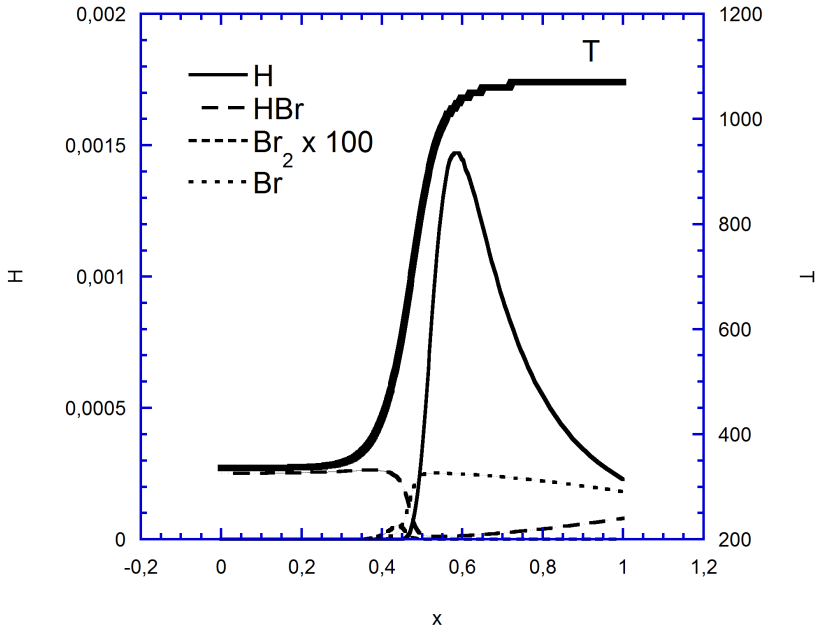

Figure 10: Predicted laminar flame structure for the $H_2/O_2/N_2$ flame of Fig. 8 with 250 ppm HBr.

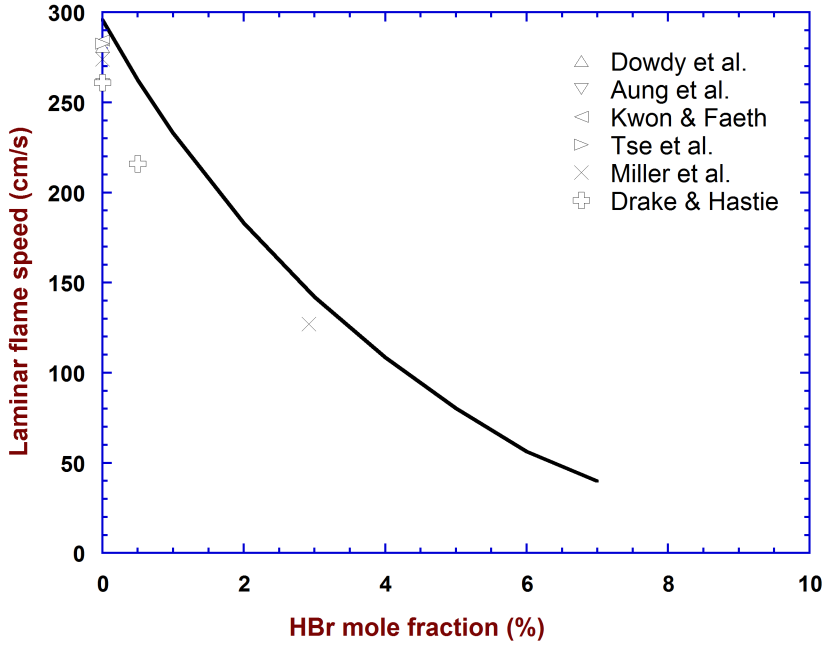

Figure 11: Comparison between measured and predicted laminar flame speeds for H_2/air/HBr mixtures at 298 K as a function of the hydrogen bromine inlet mole fraction. Symbols represent measured values, while the curves represent predictions with the current mechanism. The experimental data for the H_2/air flames are drawn from Dowdy et al. [142], Aung et al. [143], Tse et al. [144], and Kwon and Faeth [145], while the H_2/air/HBr data are taken from Miller et al. [17] and Drake and Hastie [18]. The measured flame speeds were obtained for fuel-air equivalence ratios of $1.75 \leq \phi \leq 2.0$. The calculations were conducted for an H_2/air mixture of 43.4% H_2, 11.9% O_2 and 44.7% N_2 (corresponding to $\phi = 1.875$), with varying amounts of HBr added. In the modeling, the ratios between H_2, O_2 and N_2 are kept constant; the closure is done on the sum of H_2, O_2 and N_2.

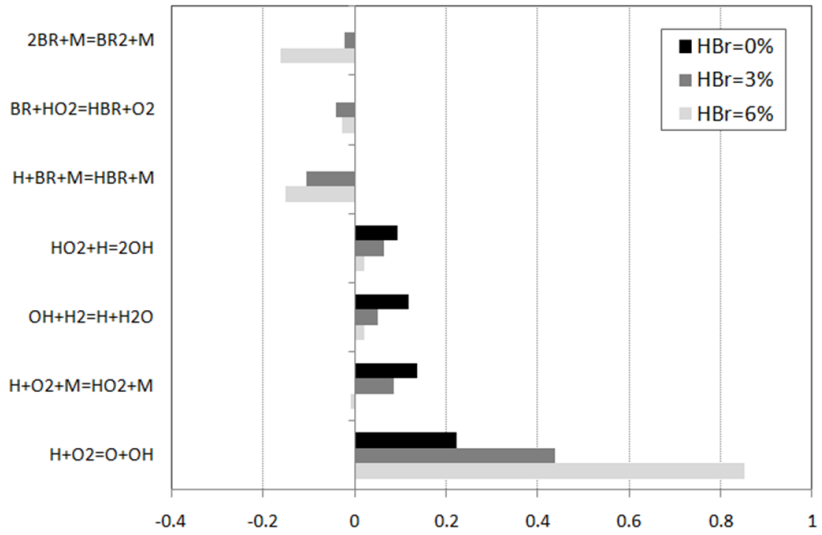

Figure 12: Linear sensitivity coefficients for the predicted laminar flame speed for H_2/air/HBr mixtures. Conditions similar to those of Fig. 11.

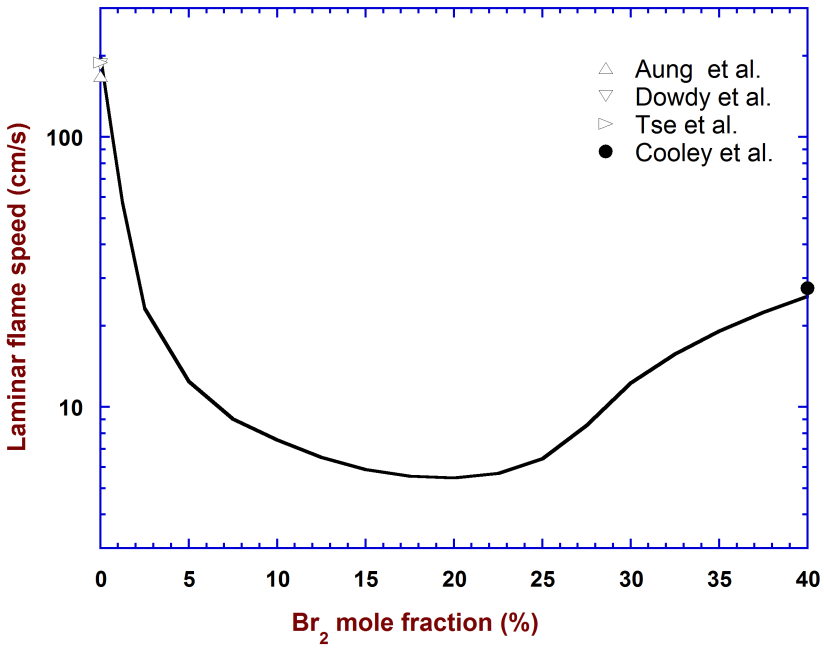

Figure 13: Predicted laminar flame speeds for H_2/air/Br_2 mixtures as a function of the air/bromine ratio (solid line). The hydrogen content of the inlet gas was maintained at 60% H_2, while the oxidizer ranged from pure air to pure molecular bromine. The inlet gas temperature was 298 K. Symbols represent measured values for H_2/air ($\phi \approx 3.5$) drawn from Dowdy et al. [142], Aung et al. [143], and Tse et al. [144], and for H_2/Br_2 (inlet temperature 322 K) drawn from Cooley et al. [132].

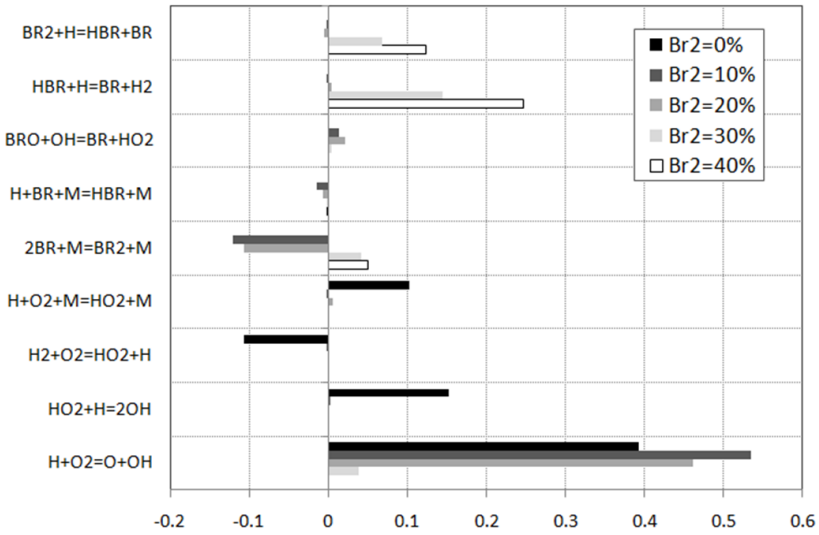

Figure 14: Linear sensitivity coefficients for the predicted laminar flame speed for H_2/air/Br_2 mixtures. Conditions similar to those of Fig. 13.